

Estimation of Ankle Joint Impedance Based on Mechanical Response During Treadmill Belt Deceleration

Yuto Oishi¹, Ayato Kanada², Motoji Yamamoto³,
Mitsuhiro Kamezaki⁴, Keisuke Yagi⁵, and Yasutaka Nakashima⁶

Abstract—The accurate estimation of ankle joint impedance during walking is crucial for understanding human gait dynamics. However, conventional methods often rely on large experimental setups or invasive techniques, which limit their practicality and accessibility. This study aimed to develop and validate a compact method for applying perturbations to the ankle joint using treadmill belt deceleration. External torque was applied to the ankle joint by rapidly decelerating the treadmill belt without prior notice to the participant. A differential model was employed to estimate the joint impedance for two participants, with the stiffness and viscosity normalized by body weight. Only models with stable poles (pole magnitude < 1) were considered. The resulting impedance estimates aligned with the expected gait-phase trends, confirming the consistency and physiological relevance of the method. This approach enables experiments to be conducted in more compact settings than those in previous studies involving large walkways. The results are comparable with previous findings, demonstrating the validity of the proposed method, which offers a practical solution for conducting gait and balance studies in constrained spaces.

I. INTRODUCTION

The control of joint stiffness, alongside that of joint angles and angular velocities [1], is crucial in all human body movements. Such regulation is achieved by actively altering the mechanical properties of the joint through the coordinated activity of its biological elements, particularly the antagonist muscle groups. Joint stiffness changes constantly, even during a single walking step, owing to muscle activity levels and the co-contraction of antagonistic muscles. The simultaneous contraction of antagonistic muscles actively increases joint stiffness from the early to mid-stance phases. Moreover, joint

This research was supported by JSPS KAKENHI Grant Numbers 23K26076 and 25K03507. The authors would like to express their gratitude.

¹Yuto Oishi is with the Graduate School of Engineering, Kyushu University, Fukuoka, Japan. oishi.yuto.205s@kyushu-u.ac.jp

²Ayato Kanada is with the Graduate School of Informatics and Engineering, The University of Electro-Communications, Tokyo, Japan.

³Motoji Yamamoto is with the Faculty of Engineering, Kyushu University, Fukuoka, Japan.

⁴Mitsuhiro Kamezaki is with the Graduate School of Engineering, The University of Tokyo, Tokyo, Japan.

⁵Keisuke Yagi is with the Graduate School of Science and Engineering, Ibaraki University, Ibaraki, Japan.

⁶Yasutaka Nakashima is with the Faculty of Engineering, Kyushu University, Fukuoka, Japan.

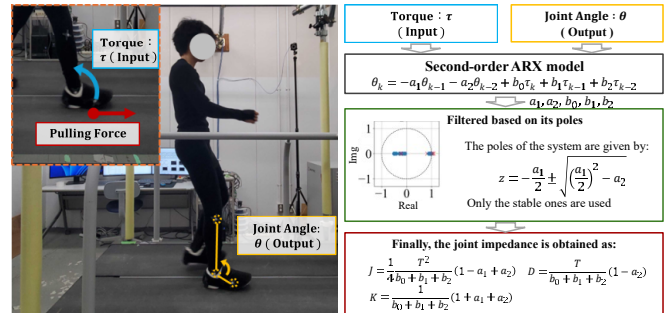


Fig. 1: External torque and angle displacement of the ankle joint after belt deceleration.

stiffness can be analyzed based on muscle activity [2]. Among the lower limb joints, the mechanical properties of the ankle joint are of particular significance. They function as the point of contact with the floor during walking, which is crucial for force transmission. This study focuses on the mechanical properties of the ankle joint, which were evaluated by joint impedance.

The joint impedance was modeled using the following equation of motion, which assumes linearity [3]:

$$\tau(t) = J(t)\ddot{\theta}(t) + D(t)\dot{\theta}(t) + K(t)\theta(t) \quad (1)$$

Here, τ is the torque applied to the joint from the outside, θ is the joint angle, $\dot{\theta}$ represents the joint angular velocity, and $\ddot{\theta}$ is the joint angular acceleration. The joint impedance J , D , and K correspond to the inertia [$\text{kg} \cdot \text{m}^2$], viscosity [$\text{Nm} \cdot \text{s}/\text{rad}$], and stiffness [Nm/rad], respectively, which are the coefficients in Eq. (1). A system identification technique was used to calculate the joint impedance. The parameters that fit the measured input/output data were the coefficients in Eq. (1), which correspond to the joint impedance.

Accurate system identification requires careful consideration of the nature of the output signals. In joint impedance estimation, the analysis is restricted to periods during which the angular response is unaffected by voluntary or reflexive components elicited by the applied perturbation.

This method necessitates the application of external torque to the joint from the outside (external torque). To date, either wearable or stationary devices have been used for this purpose. Lee et al. [4] reported the use of the rehabilitation robot Anklebot to estimate the ankle impedance during the swing phase, which is an example

of a wearable device. Owing to the device's weight of approximately 3 kg, the wearer's gait may differ from normal during the experiment, adversely affecting the accuracy of the joint impedance estimation. Rouse et al. [5] investigated ankle impedance estimation using a device that can tilt part of the walkway floor. This method offers the advantage of requiring only lightweight measurement equipment, such as an attached goniometer, to conduct experiments. However, the device requires a considerable length of 5.25 m in the walking direction. The stride length of an adult with an average height of 170 cm is approximately 0.5 m. Thus, approximately 10 steps can be taken on this device from a standing position. If external torque is applied within the 10-step interval, the participant can readily predict its timing, which may change the gait significantly. In our study, a treadmill was used to reduce the influence of the external torque predictability, addressing the spatial constraints of the walking space. Moreover, we applied the external torque by focusing on the contact between the belt and sole [6]. Continuous walking is achievable using a treadmill without the spatial restrictions associated with body movement. The overall length of the experimental device can be reduced. This approach reduces timing predictability when external torque is applied. Therefore, we aimed to estimate the joint impedance from a more natural reaction.

However, negative viscosity values were obtained in the experimental participants of Oishi et al. [6] and Rouse et al. [5]. When the viscosity value is negative, the homogeneous solution of the motion equation diverges, indicating that the mechanical energy increases over time. However, the likelihood of this phenomenon occurring during human joint movement is significantly low. Several factors may account for this; one possible explanation is the inclusion of voluntary and reflex components within the analysis range of the data. To address this issue, we describe a method for determining an identification interval that excludes these components later in this paper. Yagi et al. [7] identified the parameters using a differential model. In addition, the sign of the joint impedance was discussed based on the stability of the transfer function of the identified model. This method visualizes the stability of the identified model on the complex plane, enabling the sign of the joint impedance to be investigated, and suggests the feasibility of real-time joint impedance estimation using digital signals [8]. However, in our study, only offline estimation was performed, and the joint impedance was estimated using a differential model, with the aim of consistently yielding positive values. This method is beneficial for achieving more accurate joint impedance estimations.

This study proposes a method for estimating ankle joint impedance by applying external torque to a participant's ankle joint during treadmill walking, using a parameter identification approach based on a differential model.

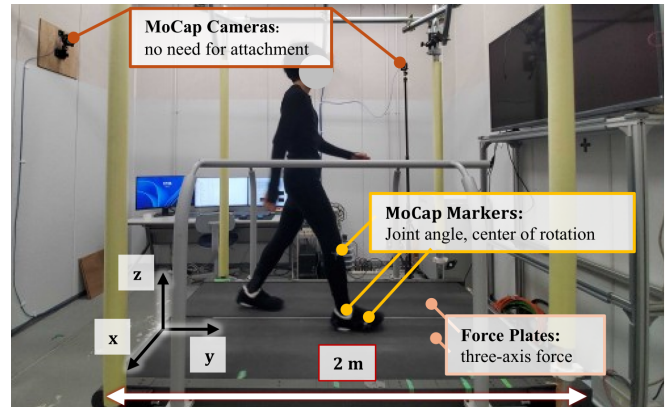


Fig. 2: Set up: motion capture and dual-belt treadmill with independent force plates.

II. METHOD

Our approach follows that of Yagi et al. [7] in employing a differential model to estimate joint impedance. The key distinctions lie in the application of external torque via a treadmill, the procedure for determining the identification interval, and the method for removing voluntary and reflex components.

A. Perturbation from Treadmill Belt Deceleration

We propose a method for applying external torque to the ankle joint by suddenly decelerating the treadmill belt without notifying the participant. This method has two major advantages. First, it can apply external torque to the joint without the participant having to wear an actuator. Fig. 1 illustrates how external torque is applied to the joint by decelerating the belt. Second, the device length is approximately 2 m, which is approximately half the size of that used in previous studies. Fig. 2 illustrates the experimental setup.

B. Algorithm for Estimating Ankle Joint Impedance

In previous studies, the joint impedance was discussed in terms of the continuous-time coefficients of Eq. (1). This study aimed to determine these parameters. To achieve this, we identified the parameters in discrete time and convert them into continuous time coefficients. The relationship between the external torque and angular displacement of the joint is expressed as a differential equation in Eq. (2). In addition, we estimated the parameters using the sampled data.

$$\theta_k = -a_1\theta_{k-1} - a_2\theta_{k-2} + b_0\tau_k + b_1\tau_{k-1} + b_2\tau_{k-2} \quad (2)$$

Here, a_1, a_2, b_0, b_1, b_2 are constants over time. k is an integer, and is expressed as $t = kT$ using the sampling period T and sampling time t .

$$\mathbf{c}^T = [a_1, a_2, b_0, b_1, b_2] \quad (3)$$

$$\mathbf{z}_k^T = [-\theta_{k-1}, -\theta_{k-2}, \tau_k, \tau_{k-1}, \tau_{k-2}] \quad (4)$$

Using Eqs. (3) and (4), Eq. (2) becomes

$$\theta_k = \mathbf{z}_k^T \mathbf{c} + r_t \quad (5)$$

where r_t is the error term. In addition, using Eq. (6), the N equations obtained for $k = 1, 2, \dots, N$ can be expressed as Eq. (7):

$$\boldsymbol{\theta} = \begin{bmatrix} \theta_1 \\ \theta_2 \\ \vdots \\ \theta_N \end{bmatrix}, \quad H = \begin{bmatrix} \mathbf{z}_1^T \\ \mathbf{z}_2^T \\ \vdots \\ \mathbf{z}_N^T \end{bmatrix}, \quad \mathbf{r} = \begin{bmatrix} r_1 \\ r_2 \\ \vdots \\ r_N \end{bmatrix} \quad (6)$$

$$\boldsymbol{\theta} = H\mathbf{c} + \mathbf{r} \quad (7)$$

Using the obtained input and output data, the system parameter vector \mathbf{c} , which minimizes the squared error expressed by Eq. (8), was determined.

$$S = \sum_{i=1}^N r_i^2 = \mathbf{r}^T \mathbf{r} = (\boldsymbol{\theta} - H\mathbf{c})^T (\boldsymbol{\theta} - H\mathbf{c}) \quad (8)$$

From the obtained differential equation parameters and sampling period, the continuous-time joint impedance J , D , and K were calculated using the following bilinear transformation:

$$J = \frac{1}{4} \frac{T^2}{b_0 + b_1 + b_2} (1 - a_1 + a_2) \quad (9)$$

$$D = \frac{T}{b_0 + b_1 + b_2} (1 - a_2) \quad (10)$$

$$K = \frac{1}{b_0 + b_1 + b_2} (1 + a_1 + a_2) \quad (11)$$

where a_1 , a_2 , b_0 , b_1 and b_2 are the coefficients that appear in Eq. (2).

C. Data Analysis

In this study, ground reaction forces and kinematic data were collected using integrated force plates built in the split-belt treadmill (Beltec, double-belt treadmill ITR-5018-11) and a motion capture system (OptiTrack TM, manufactured by OptiTrack Japan). The force plates embedded in the split-belt treadmill measure ground reaction forces separately for each foot during the steady-state walking and deceleration phases. A split-belt treadmill was used to measure ground reaction forces from the left and right feet independently, enabling the calculation of foot-specific joint torques. Force data were sampled at 1000 Hz. The motion capture system recorded the ankle joint angles and center of rotation at a sampling rate of 250 Hz. The joint impedance was estimated from the motion capture data using Eq. (2). Accordingly, the sampling interval was set to $T = 0.004$ s.

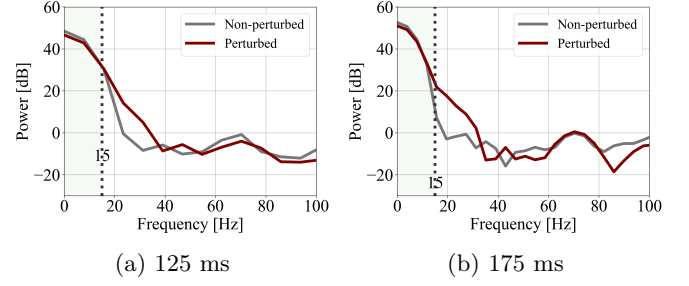


Fig. 3: Comparison of ankle angle power between perturbed and non-perturbed conditions.

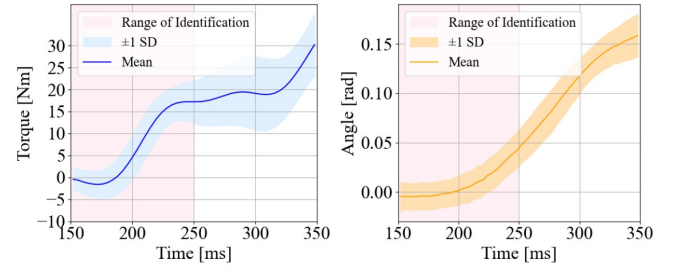


Fig. 4: Representative example of external torque and ankle joint angle displacement following belt deceleration.

D. Calculating External Torque

The ankle torque during steady walking and deceleration was calculated using Eq. (12), similarly to Rouse et al.[5].

$$\tau_{\text{model}} = F_y(Z - COP_z) + F_z(COP_y - Y) \quad (12)$$

Here, F_y and F_z are the anteroposterior and vertical ground reaction forces during walking, respectively. The origin of the coordinate system in the motion capture was also set as the origin of the system. COP_y and COP_z are the anteroposterior and vertical coordinates of the COP (center of foot pressure) during walking, respectively. Y and Z are the anteroposterior and vertical coordinates of the center of rotation of the ankle joint, respectively.

Calculating the external torque applied by the belt deceleration is crucial for estimating the joint impedance. The external torque was calculated by subtracting the walking step torque with no belt deceleration from that with deceleration, as shown in Eq. (13).

$$\tau = \tau_{\text{perturbed}} - \tau_{\text{non perturbed}} \quad (13)$$

E. Measurement of Ankle Angular Displacement

The ankle joint angle and center of rotation during steady walking and deceleration were measured using motion capture. Fig. 2 shows the markers, which were attached to the upper end of the fibula, lower end of the fibula, and outer edge near the shaft of the fifth metatarsal bone. The angle of the ankle joint was calculated from the positions of the three markers. The externally applied angle was calculated using Eq. (14).

$$\theta = \theta_{\text{perturbed}} - \theta_{\text{non-perturbed}} \quad (14)$$

F. Determining Range of Identification

Using angle data (θ) that excludes voluntary and reflex reaction components is crucial for estimating joint impedance as a mechanical property. Based on the results of a preliminary experiment, we confirmed that voluntary and reflex reaction components were clearly observed when more than 175 ms had elapsed following the deceleration command to the treadmill belt, whereas such components were not evident when the elapsed time was within 125 ms. Fig. 3 shows the power spectral analysis of the joint angle data during the 125 ms and 175 ms intervals following the treadmill deceleration command for both the non-perturbed and perturbed conditions. Compared with the 175 ms interval, the 125 ms interval exhibited smaller differences between the non-perturbed and perturbed conditions in the low-frequency range (below 15 Hz). As 99% of the power during walking exists within 15 Hz [9], the differences in this range between the two conditions are interpreted as indicating the presence of voluntary and reflex responses to the perturbation. This suggests that the contribution of voluntary and reflexive components to the input torque was minimal during the 125 ms interval. Therefore, we estimated the joint impedance using the joint angle and external torque data recorded within the first 125 ms after the treadmill deceleration command. The torque and angle data of a representative participant are shown in Fig. 4. The left edge of the graph ($= 0.15$ s) indicates the timing of the deceleration command to the treadmill.

III. EXPERIMENT

Prior to the impedance estimation experiment, we conducted an experiment to determine the treadmill belt speed and cadence to reduce gait variability. The experiment involved two men in their twenties with no history of neuromuscular disorders (Participant A: 169 cm, 55 kg; Participant B: 172 cm, 58 kg). The participants walked on a treadmill for approximately 5 min to determine a comfortable belt speed and cadence (Participant A: 1.1 m/s, 111 bpm; Participant B: 1.1 m/s, 102 bpm). During the experiment, a metronome constantly played sounds corresponding to the cadence of each participant, enabling them to maintain their target walking rhythm.

The experiment was conducted on the right ankles of the two participants. While walking on a treadmill at a constant speed of 1.1 m/s, the belt speed of the treadmill decelerated to 0 m/s with an acceleration of 10 m/s^2 . This speed condition was set based on the magnitude of forced angular displacement applied to the ankle joints of the participants in the study by Rouse et al. The impact received from the ground surface after initial contact is effectively absorbed by the ankle joint, and predictive control of the ankle joint stiffness at heel strike is a crucial

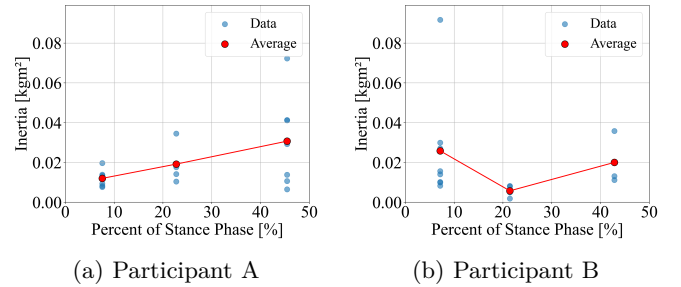


Fig. 5: Results of inertia (J).

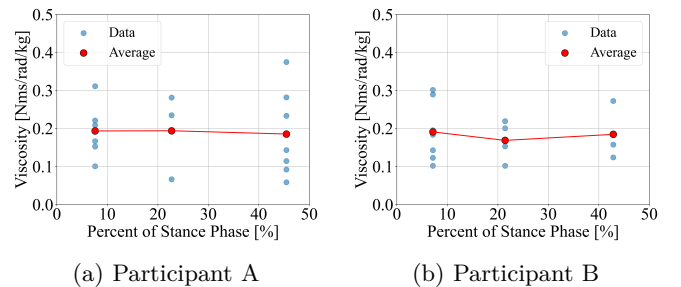


Fig. 6: Results of viscosity (D).

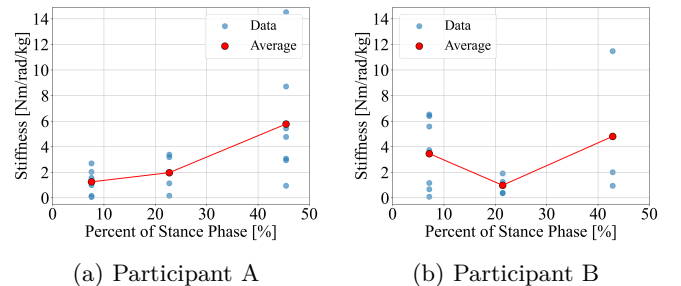


Fig. 7: Results of stiffness (K).

element of motor adaptation in human walking on a split-belt treadmill [10]. In this study, to determine the impedance of the ankle joint from the early to early mid-stance phase, the belt of the treadmill was decelerated at three different timings after the right foot landed, from the heel strike to the load response phase: i) 50 ms, ii) 150 ms, and iii) 300 ms. 10 trials were conducted at each time point. The experiment was conducted with the approval of the Kyushu University Faculty of Engineering Experimental Ethics Review Committee (Engineering Approval No. 2025-03).

IV. RESULTS

Figs. 5–7 show the joint impedance estimation results for the two experimental participants. The viscosity and stiffness values were normalized to the body weight, inertia is not normalized. Based on the pulse transfer function obtained from the identified differential model, only the models whose pole distance from the origin was < 1 (i.e., stable poles) were considered, and the joint impedance calculated from the coefficients was

plotted. The horizontal axis was set to the proportion of the stance phase corresponding to the experimental conditions i) 50 ms, ii) 150 ms, and iii) 300 ms (Participant A: i) 7.6%, ii) 22.7%, and iii) 45.5%, Participant B: i) 7.1%, ii) 21.4%, and iii) 42.9%). The scores plotted in Figs. 5-7 were as follows: i) Participant A: 6/10, Participant B: 7/10; ii) Participant A: 3/10, Participant B: 4/10; iii) Participant A: 7/10, Participant B: 3/10.

V. DISCUSSION

A. Validity Evaluation of Proposed Method

1) *Stiffness*: Previous studies have suggested that ankle joint stiffness changes throughout the gait cycle in conjunction with the state of muscle exertion during walking. Fig. 7 presents the results obtained using the proposed method. For validation, these results were compared with those reported by Rouse et al. [5] and Oishi et al. [6], as shown in Fig. 8. The results of the previous studies were plotted as data visually extracted from their graphs. Similar to the results of our previous study and those of Rouse et al., the results obtained in this study showed a tendency for the stiffness values to increase following contact with the ground. This corresponds to the increased activity of the gastrocnemius muscle during the transition to single-leg support following contact with the ground, as it supports body weight and shifts the center of gravity. This was considered to be a reasonable trend. The comparison of the stiffness values obtained in this study indicate that the results are similar to those of Rouse et al., rather than to those of our previous study.

2) *Inertia*: The moment of inertia of the two participants was calculated based on a report by Winter [11], which was approximately 0.018 kgm^2 . The estimated results presented in Fig. 5 are in agreement with this value, suggesting the validity of the results. The values did not change significantly between conditions i), ii), and iii), suggesting that only minor fluctuations occurred in response to changes in muscle activity.

3) *Viscosity*: Finally, no negative viscosity values were obtained in our proposed method. We consider that the viscosity values estimated over the gait cycle in previous studies, as well as their trends, lacked sufficient evidence of a clear association with muscle activity. Therefore, no direct comparison with these previous results was performed. However, in this study, the viscosity values were estimated simultaneously using the same data as the inertia and stiffness values. They were generally correct; moreover, the results were obtained using a method that considered the stability of the identified model. Therefore, a generally reasonable viscosity value was also obtained.

In conclusion, a joint impedance estimation method based on a differential model that applies external torque using treadmill belt deceleration is generally suitable. We obtained equivalent results in a smaller space than that

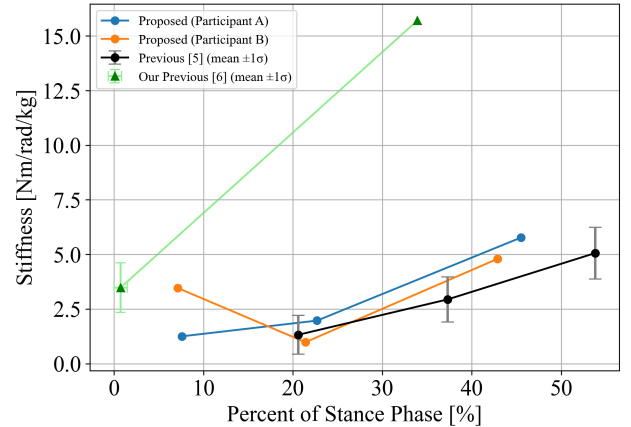


Fig. 8: Comparison of stiffness results with those of previous studies.

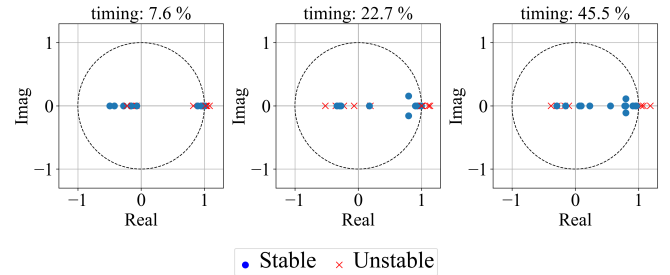


Fig. 9: Poles of the model from this experiment (Participant A).

used by Rouse et al., suggesting the effectiveness of this method.

B. Future Work

Fig. 9 shows the results of plotting the poles of the pulse transfer function calculated for all models, including the unstable poles obtained from the experiment with Participant A. In this experiment, 10 trials were conducted for each of the following three timings: i), ii), and iii). The distance from the origin of the poles of the pulse transfer function of the identified model was greater than 1, and some results were not stable, as shown in Fig. 9. We attempted to adjust the deceleration conditions of the treadmill belt to apply angular displacement comparable to that reported by Rouse et al.; however, a difference of several times remained. This discrepancy may have led to the presence of unstable poles. Therefore, the deceleration parameters will be refined further to enable more accurate estimation.

VI. CONCLUSION

In this study, we applied external torque to the joint using deceleration of a treadmill belt. We aimed to estimate the impedance of the ankle joint during walking based on a differential model. We investigated the poles of the pulse transfer function of the model identified from the experiment. The results showed that the stiffness calculated from the coefficients when the distance from

the origin was < 1 showed values similar to those of previous studies. Therefore, compared with previous methods requiring large-scale and specialized equipment that limit practicality and accessibility, joint impedance estimation using treadmill deceleration can be performed effectively and efficiently in a compact setting without adversely affecting the participant's gait.

REFERENCES

- [1] J. Kim, J. H. Moon, and J. Kim, "Impedance control of human ankle joint with electrically stimulated antagonistic muscle co-contraction," *IEEE Trans. Neural Syst. Rehabil. Eng.*, vol. 29, pp. 1593–1603, 2021.
- [2] V. Joshi, E. J. Rouse, E. S. Claffin, and C. Krishnan, "How does ankle mechanical stiffness change as a function of muscle activation in standing and during the late stance of walking?," *IEEE Trans. Biomed. Eng.*, vol. 69, no. 3, pp. 1186–1193, 2022.
- [3] J. Mizrahi, "Mechanical impedance and its relations to motor control, limb dynamics, and motion biomechanics," *J. Med. Biol. Eng.*, vol. 35, pp. 1–20, 2015.
- [4] H. Lee and N. Hogan, "Time-varying ankle mechanical impedance during human locomotion," *IEEE Trans. Neural Syst. Rehabil. Eng.*, vol. 23, no. 5, pp. 755–764, 2015.
- [5] E. J. Rouse, L. J. Hargrove, E. J. Perreault, and T. A. Kuiken, "Estimation of human ankle impedance during the stance phase of walking," *IEEE Trans. Neural Syst. Rehabil. Eng.*, vol. 22, no. 4, pp. 870–878, 2014.
- [6] Y. Oishi et al., "Estimating Lower Limb Impedance during Gait Using Treadmill-Induced Perturbations," in *Proc. 2024 IEEE Int. Conf. Robotics and Biomimetics*, pp. 494–498, 2024.
- [7] K. Yagi and H. Mochiyama, "On the determination of mapping rule and sampling interval for human joint impedance estimation," in *Proc. 2017 Annual Conf.*, pp. 1357–1362, 2017.
- [8] K. Yagi, "A Wearable Device for Ankle Impedance Estimation During Walking," in *Proc. 2024 Annual Int. Conf. IEEE Eng. Med. Biol. Soc. (EMBC)*, pp. 1–5, 2024.
- [9] E. K. Antonsson and R. W. Mann, "The frequency content of gait," *Biomech.*, vol. 18, no. 1, pp. 39–47, 1985.
- [10] T. Ogawa, N. Kawashima, T. Ogata, and K. Nakazawa, "Predictive control of ankle stiffness at heel contact is a key element of locomotor adaptation during split-belt treadmill walking in humans," *J. Neurophysiol.*, vol. 111, no. 4, pp. 722–732, 2014.
- [11] David A. Winter, "Biomechanics and Motor Control of Human Movement (fourth edition)," Wiley, 2009.